IOPscience iopscience.iop.org

Home Search Collections Journals About Contact us My IOPscience

Neutrino emission from nearby supernova progenitors

This content has been downloaded from IOPscience. Please scroll down to see the full text.

2016 J. Phys.: Conf. Ser. 718 062073

(http://iopscience.iop.org/1742-6596/718/6/062073)

View the table of contents for this issue, or go to the journal homepage for more

Download details:

IP Address: 130.54.110.33
This content was downloaded on 14/03/2017 at 00:11

Please note that terms and conditions apply.

You may also be interested in:

First neutrinos for US experiment

THE PROGENITOR OF SN 1987A
Philipp Podsiadlowski

China to open underground neutrino experiment
Jiao Li

Neutrinos at extreme energies
Roberto Aloisio

Self-interacting dark matter and sterile neutrinos
Yong Tang

Neutrino properties from cosmology
Licia Verde

Journal of Physics: Conference Series **718** (2016) 062073 doi:10.1088/1742-6596/718/6/062073

Neutrino emission from nearby supernova progenitors

Takashi Yoshida[1,2], **Koh Takahashi**[1], **Hideyuki Umeda**[1]

[1]Department of Astronomy, Graduate School of Science, University of Tokyo, 7-3-1 Hongo, Bunkyo-ku, Tokyo 113-0033, Japan
[2]Yukawa Institute for Theoretical Physics, Kyoto University, Kitashirakawa-Oiwakecho, Sakyo-ku, Kyoto 606-8502, Japan

E-mail: `tyoshida@astron.s.u-tokyo.ac.jp`

Abstract. Neutrinos have an important role for energy loss process during advanced evolution of massive stars. Although the luminosity and average energy of neutrinos during the Si burning are much smaller than those of supernova neutrinos, these neutrinos are expected to be detected by the liquid scintillation neutrino detector KamLAND if a supernova explosion occurs at the distance of ∼100 parsec. We investigate the neutrino emission from massive stars during advanced evolution. We calculate the evolution of the energy spectra of neutrinos produced through electron-positron pair-annihilation in the supernova progenitors with the initial mass of 12, 15, and 20 $M_\odot$ during the Si burning and core-collapse stages. The neutrino emission rate increases from $\sim 10^{50}$ s^{-1} to $\sim 10^{52}$ s^{-1}. The average energy of electron-antineutrinos is about 1.25 MeV during the Si burning and gradually increases until the core-collapse. For one week before the supernova explosion, the KamLAND detector is expected to observe 12–24 and 6–13 $\bar{\nu}_e$ events in the normal and inverted mass hierarchies, respectively, if a supernova explosion of a 12–20 $M_\odot$ star occurs at the distance of 200 parsec, corresponding to the distance to Betelgeuse. Observations of neutrinos from SN progenitors have a possibility to constrain the core structure and the evolution just before the core collapse of massive stars.

1. Introduction

Supernova (SN) explosion is a final event of massive star evolution. From C-burning, the energy generated by nuclear burning in massive stars is mainly carried out by neutrinos. The neutrino luminosity becomes larger and the evolution time scale becomes shorter as the evolution proceeds. The neutrino luminosity becomes $\sim 10^{47}$ erg s^{-1} during the Si burning. Although this luminosity value is still much smaller than that of SN neutrinos ($L_\nu \sim 10^{53}$ erg s^{-1}), the current neutrino detectors are expected to detect these neutrinos if a SN explosion occurs at a distance of ∼100 parsec from the earth. One candidate is Betelgeuse, a red supergiant with the initial mass of $15 - 18 M_\odot$. The distance to the star is 197 ± 45 parsec [1].

In order to predict the neutrino events from a SN progenitor before the SN explosion, one needs to evaluate neutrino spectra during the advanced evolution of massive stars. The spectra of neutrinos produced through pair neutrino process [2, 3] and plasma neutrinos [4] for typical temperatures and densities in burning processes, and weak interactions in iron core [5] has been evaluated. Neutrino events of a 15 $M_\odot$ SN progenitor by the current and future neutrino detectors were also investigated [6]. Properties of the neutrinos from a progenitor of an electron-capture SN are compared to those of progenitors of normal core-collapse SNe [7].

Content from this work may be used under the terms of the Creative Commons Attribution 3.0 licence. Any further distribution of this work must maintain attribution to the author(s) and the title of the work, journal citation and DOI.
Published under licence by IOP Publishing Ltd

Table 1. Properties of stellar evolution models. The masses are shown in the unit of the solar mass ($M_\odot$).

$M_{\rm init}$	$M_{\rm fin}$	$M_{\rm CO}$	$M_{\rm Fe}$	$t_{\rm Si-b}$ (days)	$t_{\rm col}$ (hours)
12	10.6	1.82	1.28	8.6	30.0
15	12.3	2.74	1.49	4.4	21.4
20	14.3	4.64	1.44	1.1	10.4

The detectability of the neutrino events from SN progenitors by the liquid scintillator detector KamLAND was discussed [8]. They expected that KamLAND can detect neutrino events of a 25 $M_\odot$ SN progenitor at a distance less than 660 parsec.

In this study, we investigate the time evolution of the spectra of neutrinos emitted through pair neutrino process from SN progenitors during the stages from the Si burning to the core-collapse. We evaluate the neutrino events of SN progenitors with the initial mass of 12, 15, and 20 $M_\odot$ by KamLAND.

2. Calculation method

2.1. Stellar evolution model

We calculate the evolution of massive stars with the initial mass $M_{\rm init}$ of 12, 15, and 20 $M_\odot$ from the H-burning to the time when the central temperature reaches $T_{\rm C} = 6.5 \times 10^9$ K. We use the stellar evolution code in [9] with the extended nuclear reaction network consisting of 300 species of nuclei. Table 1 shows the final mass $M_{\rm fin}$, CO core mass $M_{\rm CO}$ and Fe core mass $M_{\rm Fe}$ at the final step, the interval from the ignition of the core Si burning to the last step $t_{\rm Si-b}$, and the interval from the end of the core Si burning to the last step $t_{\rm col}$. Here we define the ignition of the core Si burning when the stellar center becomes convective. The end of the core Si burning is defined as the time when the central convection turns off.

In these models, the final mass and CO-core mass correlate with the initial stellar mass but the Fe-core mass is not. The period of the Si burning is a half day (20 $M_\odot$ model) to one week (12 $M_\odot$ model). The period also depends on the stellar mass. After the central Si exhaustion, the formed Fe core collapses within about one day.

2.2. Evaluation of neutrino spectra

During advanced stages of massive star evolution, a main neutrino emission process is electron-positron pair annihilation (pair neutrino process) (e.g., [7]). This process emits neutrinos and antineutrinos with all flavors. On the other hand, electron capture of Fe-peak elements dominates the neutrino emission in the collapsing stage. However, this process emits mainly only electron neutrinos and, thus, the detectability by the current neutrino detectors such as Super-Kamiokande and KamLAND is expected to be smaller than that of electron antineutrinos. Here, we calculate the spectra of neutrinos and antineutrinos emitted by pair neutrino process.

We calculate the neutrino spectra using the formulation of the reaction rate of pair neutrino process in [10]. The integration of electron and positron distribution functions in the momentum space is performed with Monte Carlo simulation. We construct a table of neutrino spectra as a function of the temperature and the electron number density. When we evaluate the neutrino spectra of a star at each time step, first we calculate the spectra in the unit mass of each mass coordinate having the values of the temperature and electron number density with interpolating the values in the table. Then, we deduce the neutrino spectra of the step by integrating the spectra in the mass coordinate.

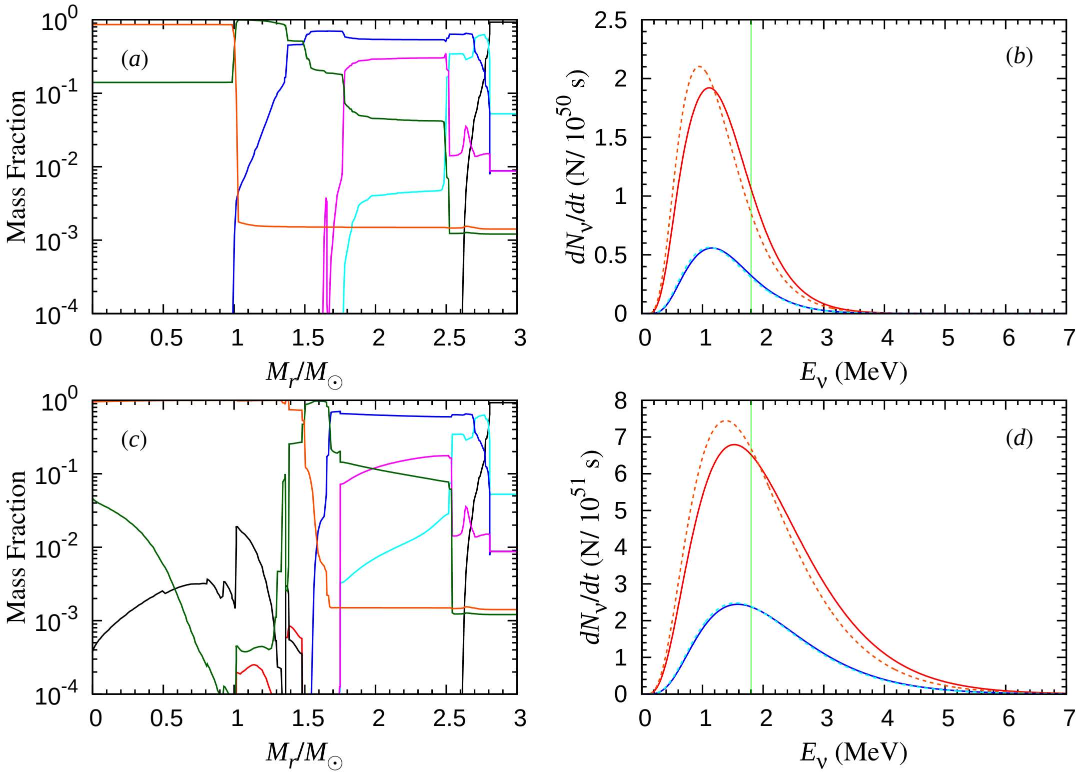

Figure 1. Panels (a) and (b) show the mass fraction distribution and the neutrino energy spectra of the 15 $M_\odot$ model in the core Si burning, respectively. Panels (c) and (d) show those at the last step. In panels (a) and (c), red, black, skyblue, blue, purple, green, and orange lines indicate the mass fractions of ^{1}H, ^{4}He, ^{12}C, ^{16}O, ^{20}Ne, "Si", and "Fe". In panels (b) and (d), red solid, orange dashed, blue solid, and skyblue dashed lines indicate the spectra of ν_e, $\bar{\nu}_e$, $\nu_{\mu,\tau}$, and $\bar{\nu}_{\mu,\tau}$. The green vertical lines indicate the threshold neutrino energy of KamLAND.

3. Results

3.1. Neutrino emission from a 15 $M_\odot$ SN progenitor

We will show the spectra of neutrinos emitted by pair neutrino process during the core Si burning and at the last step of the calculation of the 15 $M_\odot$ SN progenitor. Four panels of Fig. 1 show the mass fraction distribution of the central region and the neutrino spectra. Panel (a) indicates the mass fraction distribution at 1.15 days before the last step. The star is in the core Si burning stage. The central temperature and density are $T_{\rm C} = 3.6 \times 10^9$ K and $\rho_{\rm C} = 5.2 \times 10^7$ g cm^{-3}. The mass fractions of the intermediate elements from Si to Sc, denoted by "Si", and heavier Fe-peak elements, denoted by "Fe", are 0.14 and 0.86, respectively, at the center. The intermediate elements such as Si and S burn into Fe-peak elements in the central core and the Fe-rich core grows up. On the Fe core, Si/O, O/Si, O/Ne, O/C, C/O, and He/C layers are surrounded.

Panel (b) indicates the neutrino spectra during the core Si burning. The neutrino emission rate during the Si burning is the order of 10^{50} s^{-1}. The emission rate gradually increases in the burning stage. The average $\bar{\nu}_e$ energy is 1.25 MeV. This energy is smaller than 1.8 MeV, the threshold energy of $\bar{\nu}_e + p \to n + e^+$, so that only a part of high energy tail will be detected by neutrino detectors. The spectra of ν_e and ν_x are slightly larger than $\bar{\nu}_e$ and $\bar{\nu}_{\mu,\tau}$, respectively. This is because electrons generally have higher energy distribution than positrons in the stellar interior and the forward emission of neutrinos (not antineutrinos) against electrons is favored [11]. Neutrinos are mainly produced in the central region.

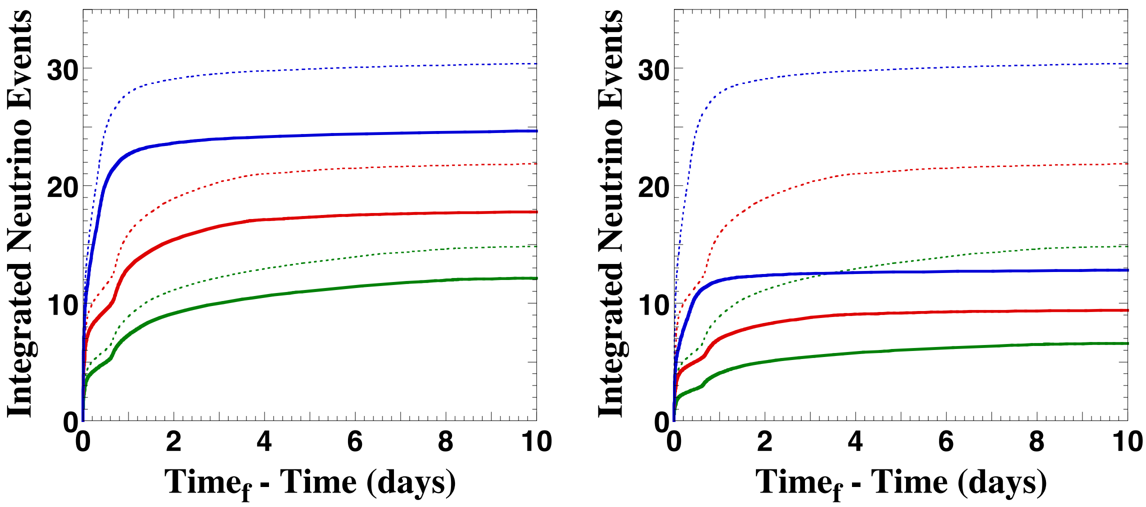

Figure 2. Integrated neutrino events from a given time to the last step of the stellar evolution calculation. Left and right panels correspond to the normal and inverted mass hierarchies, respectively. Solid lines are the case where the neutrino oscillation is taken into account and dotted lines are the case where it is not. The green, red, and blue lines indicate the neutrino events of the 12, 15, and 20 $M_\odot$ models.

At the last step, the temperature and density increase to 6.5×10^9 K and 3.0×10^9 g cm^{-3} (panels (c) and (d)). The Fe-core mass becomes 1.49 $M_\odot$. The neutrino emission rate increases to $\sim 10^{52}$ s^{-1}. The peak energy of each neutrino spectrum becomes close to the threshold energy. The average $\bar{\nu}_e$ energy is 1.94 MeV. Neutrinos are mainly emitted from the outer region of Fe core ($M_r \sim$ 1–1.2 $M_\odot$). The neutrino emission from the central region is subdominant because the central density becomes high and the effect of electron degeneracy appears.

3.2. Neutrino events by KamLAND
KamLAND is a 1 kiloton liquid scintillation neutrino detector [12]. If a SN explosion occurs, electron antineutrinos will be detected through $\bar{\nu}_e + p \rightarrow n + e^+$ by KamLAND. After this neutrino reaction, the 2.2 MeV γ-rays emitted by the following reaction $n + p \rightarrow d + \gamma$ will be detected. Thus, KamLAND detects neutrinos with the threshold energy of 1.8 MeV. Owing to this low energy threshold, KamLAND is expected to make it possible to detect neutrinos from the progenitors of nearby SNe.

We evaluate the neutrino events of the SN progenitors of 12, 15, and 20 $M_\odot$ by KamLAND. We assume that the distance to a SN is 200 parsec, corresponding to the distance to Betelgeuse. The proton number of the KamLAND detector is set to be 5.98×10^{31} [12]. For simplicity, we do not consider the detection efficiency and the energy resolution. We adopt the cross section of the neutrino reaction $\bar{\nu}_e + p \rightarrow n + e^+$ in [13]. Neutrinos change their flavors by the MSW effect while they leave the star. We assume that the transition probability of $\bar{\nu}_e \rightarrow \bar{\nu}_e$ is 0.68 and 0.02 in the normal and inverted mass hierarchies, respectively.

Figure 2 shows the integrated neutrino events from a given time to the last step of the stellar evolution. This figure is an indicator of neutrino events observed before a SN explosion. For example, we will observe 13 and 17 neutrino events for one and three days before the SN explosion of the 15 $M_\odot$ model in the normal mass hierarchy. In the normal mass hierarchy, the evaluated $\bar{\nu}_e$ events for one week before the explosion are 12, 18, and 24 for 12, 15, and 20 $M_\odot$ models, respectively. The expected $\bar{\nu}_e$ event number is larger for more massive model. In addition, the increase in the neutrino event becomes steeper just before the end of the evolution. This relates to shorter period of the Si burning for more massive star. In the inverted mass hierarchy, the evaluated events for one week are 6, 9, and 13 for 12, 15, and 20 $M_\odot$ models. Since the emission rate of $\bar{\nu}_e$ is larger than $\bar{\nu}_{\mu,\tau}$ and the transition probability of $\bar{\nu}_e$ to $\bar{\nu}_e$ in the normal mass hierarchy is larger than the inverted mass hierarchy, the number of the $\bar{\nu}_e$ events in the normal mass hierarchy is larger. The event number and the detection time scale of neutrinos from a SN progenitor depend on the progenitor mass. The neutrino observations of SN progenitors will provide constraints to the initial mass and the core mass of the SN progenitors.

We see less steep locations in about 0.7 day to the last step in the 12 and 15 $M_\odot$ models. At this time, the core Si burning has finished and the O-shell burning ignites. The dominant neutrino emission region changes from the center to the location of the O/Si-layer. Furthermore, the central temperature decreases. Since the temperature of the O/Si-layer is lower than the central temperature, the average neutrino energy decreases. The small average energy reduces the neutrino reaction rate and, thus, the detection rate of $\bar{\nu}_e$ by KamLAND decreases. The decrease in the neutrino event rate relates to the change of the burning processes in the central region during the collapsing stage of massive stars. In practice, it will be difficult to find such a time variation of the neutrino event rate from the expected small events. However, we may observe the change of burning processes in the central region of SN progenitors with neutrino signals using a larger-size neutrino detector in future.

4. Summary

We investigated the evolution of the neutrino spectra from the Si burning to the core-collapse stage of the SN progenitors with the initial mass of 12, 15, and 20 $M_\odot$. The neutrino emission rate and the average $\bar{\nu}_e$ energy are the order of 10^{50} s^{-1} and $\sim$1.2 MeV, respectively, during the Si burning and increase to the core-collapse. If a SN explosion of a 12–20 $M_\odot$ star occurs at the distance of 200 parsec, the neutrino event number detected by KamLAND during the last one week before the core-collapse is expected to be 12–24 and 6–13 in the normal and inverted mass hierarchy. The observations of the number and time scale of the neutrino events from SN progenitors will constrain the core structure and evolution of SN progenitors.

Acknowledgments

This work has been partly supported by the grand-in-aid for Scientific Research (26104007, 26400271) from the MEXT of Japan.

References

[1] Harper G M, Brown A and Guinan E F 2008 *Astrophys. J.* **135** 1430
[2] Odrzywolek A, Misiaszek M and Kutschera M 2004 *Astropart. Phys.* **21** 303
[3] Misiaszek M, Odrzywolek A and Kutschera M 2007 *Phys. Rev.* D **74** 043006
[4] Odrzywolek A 2007 *Eur. Phys. J.* C **74** 043006
[5] Odrzywolek A 2009 *Phys. Rev.* C **80** 045801
[6] Odrzywolek A, Misiaszek M and Kutschera M 2007 *NNN06: Next Generation Nucleon Decay and Neutrino Detectors 2006, AIP Conf. Proc.* vol 944 (Americal Institute of Physics) p 109
[7] Kato C, Azari M D, Yamada S, Takahashi K, Umeda H, Yoshida T and Ishidoshiro K 2015 *Astrophys. J.* **808** 168
[8] Asakura K *et al* 2015 arXiv:1506.01175
[9] Takahashi K, Yoshida T, Umeda H, Yamada S and Sumiyoshi K 2015 *Mon. Not. R. Astron. Soc.* **456** 1320
[10] Yakovlev D G, Kaminker A D, Gnedin O Y and Haensel P 2001 *Phys. Rep.* **354** 1
[11] Buras R, Janka H Th, Keil M Th, Raffelt G G and Rampp M 2003 *Astrophys. J.* **587** 320
[12] Gando A *et al* 2013 *Phys. Rev. D* **88** 033001
[13] Strumia A and Vissani F 2003 *Phys. Lett. B* **564** 42